

RESEARCH ARTICLE

Open Access



The safe zone of distal fibula was determined based on the classification of lateral malleolus fossa

Gui-xuan You^{1†}, Lei Huang^{1†}, Ming-hui Li^{1†}, Bin Xiong², Wan-lin Peng³, Hou-yin Shi⁴ and Lei Zhang^{4,5*}

Abstract

Background Lateral malleolus fractures are very common, and the distal fibular geometry is complex. This study aimed to classify the lateral malleolus fossa (MF) into different types by characterizing the lateral MF imaging morphology and exploring the relationship between the lateral MF and internal fixation position after distal fibula fractures.

Methods Anteroposterior CT reconstruction was performed on 248 subjects. After reconstruction, the deepest point of the lateral MF was located, and then, the cross-sectional shape of the lateral MF was observed and classified.

Results According to the morphology of the CT cross section, the lateral MF was divided into three types: type C (43.1%), type V (32.2%), and type Flat (24.7%). Type V (3.98 ± 0.82) was significantly longer than type C (2.83 ± 0.54) and type Flat (1.84 ± 0.42) in cd. Similarly, in $\angle\alpha$, Type Flat (136.31 ± 9.63) was the largest, followed by type C (116.51 ± 8.79), and type V (89.31 ± 9.07) was the smallest. Other measurements were not found any significant differences between the above.

Conclusion According to the morphology of the CT cross section, the lateral MF was divided into three types: type C, type V and type Flat. Type V is most likely to be invaded when fixing the distal fibula. Screws less than 9 mm should be selected when fixing, and screws no more than 10 mm should be selected when there are type C and type Flat of MF.

Keywords Lateral malleolar fossa, Fibular fracture, Internal fixation, Ankle

[†]Gui-xuan You, Lei Huang, Ming-hui Li contributed equally to this work and share first authorship

*Correspondence:

Lei Zhang
zhanglei870722@126.com

¹ School of Physical Education, Southwest Medical University, Luzhou 646000, China

² School of Clinical Medicine, Southwest Medical University, Luzhou 646000, China

³ Department of Medical Imaging, Southwest Medical University, Luzhou 646000, China

⁴ Department of Orthopedics, The Affiliated Traditional Chinese Medicine Hospital of Southwest Medical University, Luzhou 646000, China

⁵ Center for Orthopedic Diseases Research, The Affiliated Traditional Chinese Medicine Hospital of Southwest Medical University, Luzhou 646000, China



© The Author(s) 2023. **Open Access** This article is licensed under a Creative Commons Attribution 4.0 International License, which permits use, sharing, adaptation, distribution and reproduction in any medium or format, as long as you give appropriate credit to the original author(s) and the source, provide a link to the Creative Commons licence, and indicate if changes were made. The images or other third party material in this article are included in the article's Creative Commons licence, unless indicated otherwise in a credit line to the material. If material is not included in the article's Creative Commons licence and your intended use is not permitted by statutory regulation or exceeds the permitted use, you will need to obtain permission directly from the copyright holder. To view a copy of this licence, visit <http://creativecommons.org/licenses/by/4.0/>. The Creative Commons Public Domain Dedication waiver (<http://creativecommons.org/publicdomain/zero/1.0/>) applies to the data made available in this article, unless otherwise stated in a credit line to the data.

Background

The fibula is a long bone in the lower extremity that is positioned on the lateral side of the tibia. The distal end of the fibula forms the lateral malleolus which articulates with the lateral talus, creating part of the lateral ankle [1]. The lateral malleolus fossa (MF) is located in the posteromedial part of the distal fibula and is the insertion point of the posterior talofibular ligament [2]. In addition, the lateral MF is also the anatomical structure of the posterolateral talus and subtalar joint motion space [3].

Ankle fractures account for approximately 20% of extremity fractures; most ankle fractures involve the fibula. Isolated fibula fractures accounted for 55–70% of ankle fractures, bimalleolar fractures 4–20%, and trimalleolar fractures 10–11% [4–7]. Ankle fracture instability usually requires surgical treatment. In recent years, the main methods of internal fixation have included posterolateral plate fixation, locking plate construction, intramedullary instruments, etc. [8–10] No matter which internal fixation method is selected, most of the lateral malleolus fractures will pass through the distal fibula. Many scholars have explored the safe range of fibula intramedullary nail fixation and analyzed the shape, diameter, and length of the tip of the fibula [11, 12]. At the same time, the anatomical study of the lateral MF can make the placement of ligament binding screws or/and fibular plates more reasonable [11]. Furthermore, some scholars judge whether the distal fibula fracture was reduced by evaluating the fibular notch [13]. There is evidence that the geometry of the distal fibula is complex because there are many ligaments attached to the anterolateral side, and there are many studies on the anatomical structure of the innominate tuberosity of the fibula, the anterior tuberosity of the fibula and the tip of the fibula [2, 14, 15]. When fixing the lateral malleolus fracture, we found that the morphological characteristics of the lateral MF are unique. In this context, understanding the anatomical structure of the MF has a particular reference value for the safe placement of internal fixation.

Our hypothesis is that computed tomography (CT) would help to understand the morphology of the distal fibula better. By observing CT three-dimensional reconstruction, we can more fully understand the anatomical characteristics of the lateral malleolus. In this study, the primary objective was to analyze the lateral MF, focusing on the shape of the lateral MF and its anatomical classification. The secondary objective was to describe the safe area of distal fibula internal

fixation according to the anatomical classification of lateral MF.

Methods

All ankle joint CT scan images were collected from the hospital, and Ethical approval was obtained. A total of 248 subjects were included in the study, including 107 females and 141 males.

Patient selection

Inclusion criteria: (1) 18–70 years old; (2) CT images of the distal fibula and the lateral MF; (3) distal fibula fractures; (4) ankle deformities.

Exclusion criteria: (1) tibiofibular syndesmosis injury; (2) distal fibula fractures; (3) ankle deformities.

Image acquisition

The German Siemens SMATOM Definitom Edge 64-slice spiral CT machine was used to scan the ankle joint of the included population. Scanning parameters: tube voltage 120 k V, tube current 280 m A, scanning angle 0, layer thickness 1.25 mm, layer spacing 0.75 mm, window level 70, window width 320. CT images of the ankle joint were obtained after scanning. In order to facilitate the subsequent calculation of the ankle motion angle model, the scanning range is less than 1/3 distal tibia. The scanned CT images are stored in JPG format.

Establishment of the three-dimensional geometric model

Mimics 21.0 software was used to extract the obtained CT data. Based on the biological anatomy of the foot and ankle, the standard foot and ankle structure model containing the ankle joint and the surrounding bones was reconstructed. The obtained geometric model file was imported into Geomagic Wrap 2021, USA, for subdivision, noise reduction, smoothing, accurate surface, and other processes to form a three-dimensional solid foot and ankle model.

Data measurement

The reconstructed model was re-imported into Mimics 21.0, and the deepest point of the lateral MF was located on the three-dimensional model, and then the morphological characteristics of the cross section were observed. The lateral MF was then carefully observed, and geometric parameters were measured. Inter-observer reliability was assessed by two authors independently. The measurement data are shown in Figs. 1, 2, and 3. We use the average length of each type as the radius to try to depict the safe area in the cross section. On the

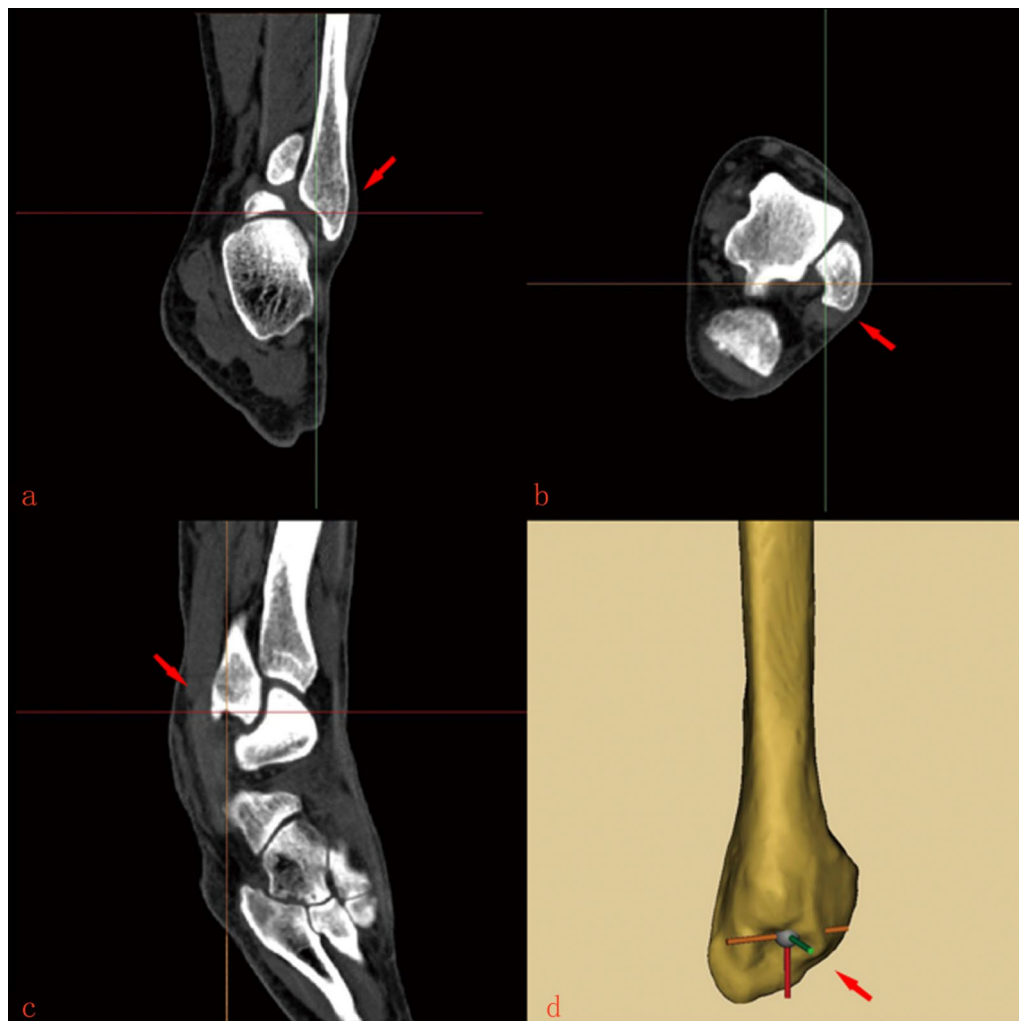


Fig. 1 Lateral MF map after three-dimensional reconstruction. **a** The frontal plane of the lateral MF location. **b** The horizontal plane of the lateral MF location. **c** The sagittal plane of the lateral MF location. **d** Three-dimensional reconstruction of the location of the lateral MF

transverse position, the upper and lower edges of the lateral fibula were taken as the center of the circle, and ab was the radius to draw the area of mutual connection. Then, the intersection of the circle and the fibular cortical bone was connected to form a closed visual image on the cross section to represent the safe range of each type of lateral MF. Finally, the CT cross section of the C-type lateral MF was used to overlap the three types of visual images, and the safety range of the internal fixation of the lateral MF was compared.

Statistical analyses

SPSS 26.0 software was used to perform statistical analysis on all the data. Since the MF is divided into three

types, the expected incidence of each type is 33%. Assuming that the allowable error is 0.05, the expected sample size is 214 by the population rate formula. Measurement data were expressed as mean \pm standard deviation. When the variance was uniform, the one-way variance was used for the analysis between groups, and Tamheini T2 (M) was used when the variance was unequal. The content of the analysis was whether there were significant differences in the measurement between the MF of different types. When $P < 0.05$, the difference was significant.

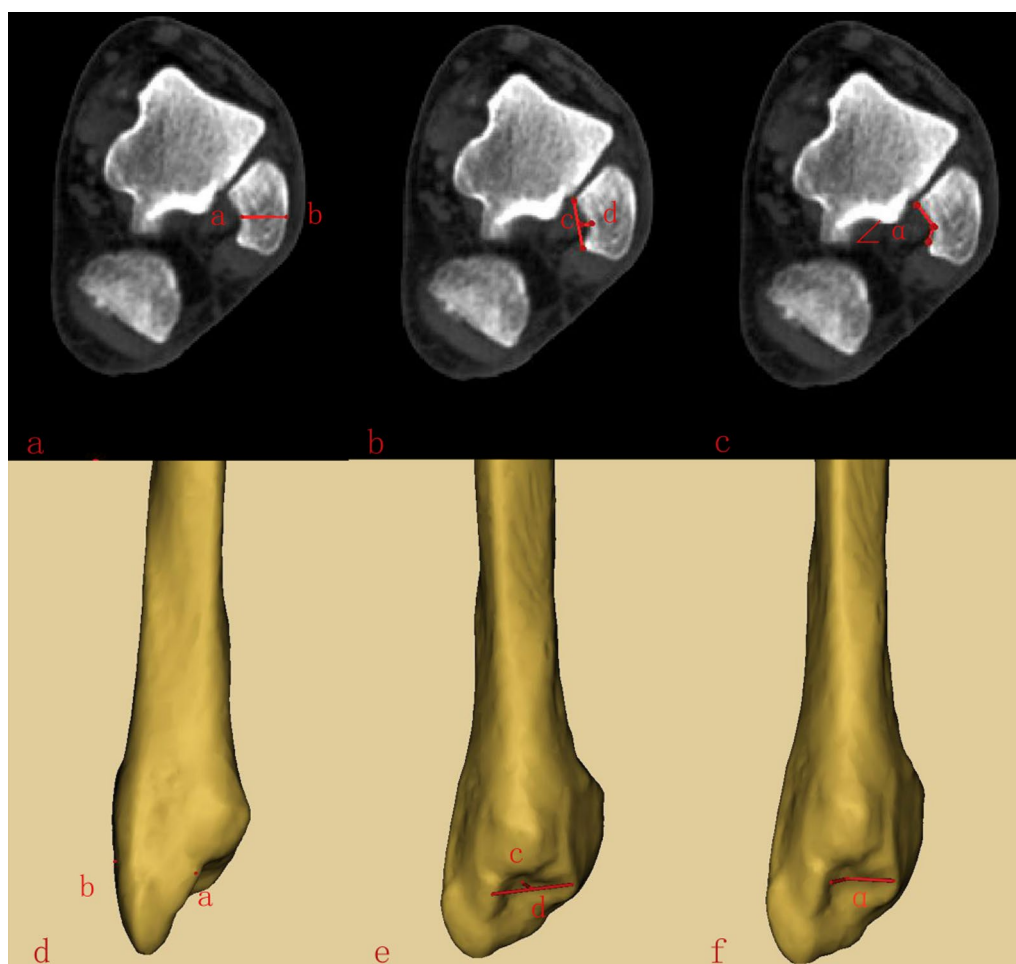


Fig. 2 Cross-sectional data measurement diagram. **a** and **d** The deepest point of lateral malleolus fibula thickness. **b** and **e** The depth of lateral MF. **c** and **f** The angle of the MF

Result

According to the combination of three-dimensional reconstruction and cross section, the lateral MF could be divided into three types: type C, type V, and type Flat, As shown in Fig. 4. Among them, type C (107, 43.1%) had the highest incidence, followed by type V (79, 32.2%). Apparently, type Flat (62, 24.7%) had the lowest proportion of all subjects. The geometric parameters corresponding to each type were measured, as shown in Table 1. Briefly, the deepest point of lateral malleolus fibular thickness in type V (3.98 ± 0.82) was significantly longer than that in type C (2.83 ± 0.54) and type Flat (1.84 ± 0.42). On the contrary, the lateral MF depth of Flat type (10.17 ± 0.77) was significantly longer than that of type C (9.69 ± 0.92)

and type V (8.54 ± 0.84). The angle of the MF of Type Flat (136.31 ± 9.63) was the largest, followed by type C (116.51 ± 8.79), and type V (89.31 ± 9.07) was the smallest. ($P < 0.05$). No statistical differences were found in other parameters. Gender and feet of left and right did not affect the classification of the MF ($P > 0.05$), as shown in Tables 2 and 3. As shown in Fig. 5, The average thickness of the fibula of different types of lateral MF was used as the baseline to delineate the safe range. Then put the safety range on the same cross section, the type V area is the smallest, while the type Flat area is the largest.



Fig. 3 Localization and measurement of lateral MF area. **3a)**The starting point of frontal area measurement. **b** The starting point of cross-sectional area measurement. **c** The starting point of sagittal area measurement. **d** ef: the length of the upper and lower surfaces of the lateral MF. gh: The left and right surface length of the outer lateral MF. s: Area size of lateral MF

Discussion

The lateral MF is on the posterolateral side of the lateral malleolus, which is the starting point of the posterior talofibular ligaments. We reconstructed 248 cases of the normal fibula and analyzed the anatomy of two-dimensional and three-dimensional images, respectively. Gandhi et al. [3] only measured the size and depth of the lateral MF without anatomical classification. We divided it into three types by the shape and angle of the transverse section of the lateral MF, among which type C has the most significant angle and

relatively large surface area. The depth of the type V shape is the largest, indicating that the thickness of the lateral malleolus is small.

Gandhi et al. [3] found that 31.5% of the lateral fibula plate had the risk of invasion of the lateral MF, and the absence of a cross-sectional scan after surgery did not determine whether the lateral MF was invaded. Short-term pain may mask the pain caused by the invasion of the lateral MF. According to research, 20% of people have unexplained ankle pain one year after ankle fracture surgery [16, 17]. The lateral MF is the attachment point of the posterior talofibular ligament and then provides

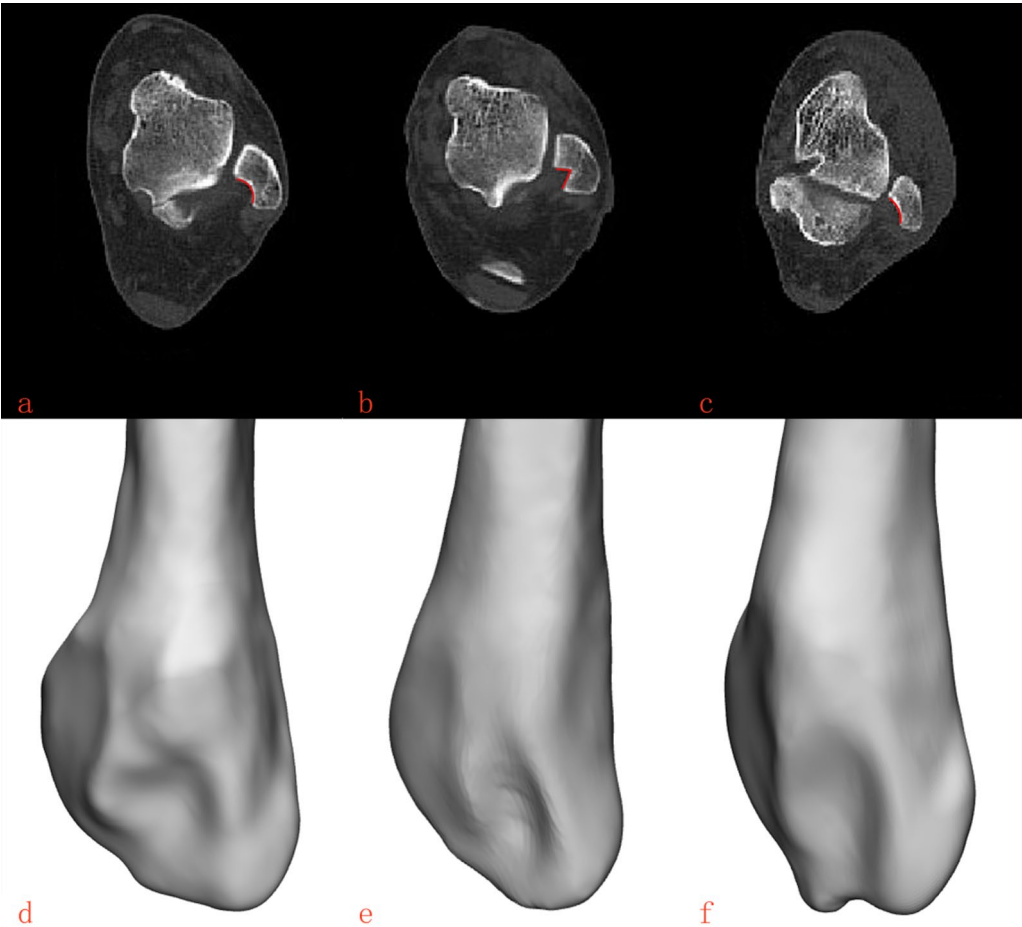


Fig. 4 The classification of lateral MF. **a** and **d** Type C of the lateral MF. **b** and **e** Type V of the lateral MF. **c** and **f** Type Flat of the lateral MF

Table 1 The geometric parameters corresponding to each type of the lateral MF

| | Type C | Type V | type flat | In total | F | P |
|----------------------|--------------|-------------|---------------|--------------|---------|-------|
| | 107 | 79 | 62 | 248 | – | – |
| ab (mm) | 9.69±0.92b | 8.54±0.84a | 10.17±0.77ab | 9.44±1.08 | 70.195 | 0.000 |
| cd (mm) | 2.83±0.54b | 3.98±0.82a | 1.84±0.42ab | 2.96±1.04 | 196.557 | 0.000 |
| ef (mm) | 12.56±1.92 | 12.32±2.05 | 12.34±2.16 | 12.43±2.02 | 0.058 | 0.994 |
| gh (mm) | 8.51±1.63 | 8.73±1.73 | 8.65±1.68 | 8.61±1.66 | 0.382 | 0.683 |
| <α(°) | 116.51±8.79b | 89.31±9.07a | 136.31±9.63ab | 112.80±20.08 | 479.020 | 0.000 |
| S (mm ²) | 84.71±23.67 | 83.49±28.31 | 86.21±29.87 | 84.20±26.72 | 0.047 | 0.954 |

a versus Type C, P<0.05; b versus Type V, P<0.05

Table 2 Classification and measurement of the lateral MF of sex

| Items | Male | Female | In total | F | P |
|----------------------|----------------|----------------|----------------|-------|-------|
| | 139 | 109 | 248 | – | – |
| ab (mm) | 9.52 ± 1.08 | 9.39 ± 1.07 | 9.44 ± 1.08 | 0.024 | 0.876 |
| cd (mm) | 3.03 ± 0.99 | 2.87 ± 1.10 | 2.96 ± 1.04 | 1.349 | 0.247 |
| ef (mm) | 12.57 ± 2.10 | 12.23 ± 1.90 | 12.43 ± 2.02 | 1.751 | 0.187 |
| gh (mm) | 8.61 ± 1.76 | 8.61 ± 1.54 | 8.61 ± 1.66 | 0.111 | 0.739 |
| <α(°) | 112.23 ± 18.86 | 113.55 ± 21.64 | 112.80 ± 20.08 | 0.262 | 0.609 |
| S (mm ²) | 83.86 ± 26.58 | 85.67 ± 26.58 | 84.20 ± 26.72 | 0.027 | 0.870 |

Table 3 Classification and measurement of the lateral MF of feet of right and left

| Items | Right | Left | In total | F | P |
|----------------------|----------------|----------------|----------------|-------|-------|
| | 137 | 111 | 248 | – | – |
| ab (mm) | 9.45 ± 1.05 | 9.43 ± 1.11 | 9.44 ± 1.08 | 0.170 | 0.895 |
| cd (mm) | 3.02 ± 0.99 | 2.89 ± 1.10 | 2.96 ± 1.04 | 1.349 | 0.247 |
| ef (mm) | 12.53 ± 2.06 | 12.29 ± 1.97 | 12.43 ± 2.02 | 0.882 | 0.349 |
| gh (mm) | 8.69 ± 1.67 | 8.53 ± 1.65 | 8.61 ± 1.66 | 0.555 | 0.457 |
| <α(°) | 112.41 ± 20.29 | 113.27 ± 19.89 | 112.80 ± 20.08 | 0.114 | 0.947 |
| S (mm ²) | 83.43 ± 26.07 | 86.83 ± 25.06 | 84.20 ± 26.72 | 1.080 | 0.300 |

some space for ankle plantar flexion and valgus. The invasion of the lateral MF may lead to plantar flexion or valgus impingement syndrome, which eventually evolves into ankle osteoarthritis.

The authors speculate that the type of ankle fracture and inferior tibiofibular fixation may be the main causes of lateral MF invasion. For example, Lauge-Hansen supination external rotation, pronation abduction, and combined ankle fracture need internal fixation or multiple screw placement near lateral MF, which increases the risk of lateral MF invasion. In addition to the location and number of internal fixators, the important factor of lateral MF invasion may be the size of itself. Larger or deeper MF is more likely to be invaded. We found that the average area of the MF was 84.2 mm², accounting for 80% of the medial area of the distal fibula; the average distance from the deepest point of the MF to the lateral fibula was about 2.96 mm, accounting for 32.7% of the fibula depth. We founded that in the same case, the greater the depth

of the type V and the smaller the fibula thickness, the greater the risk of MF invasion. Therefore, the shape of the MF should be considered when the fixation screw is placed from the outside of the distal fibula. The type V should not exceed 8 mm; otherwise, a very large wind invades the lateral MF. If it is other types, no more than 10 mm screws can be selected. At the same time, in order to verify whether the implant depth was completely guaranteed not to invade the lateral malleolus fossa, we divide the safety range by the thickness of the fibula corresponding to the type V, type C, and Type Flat, which is 8 mm, 9 mm, and 10 mm, respectively. As shown in Fig. 5, when we put the three safety ranges on the same plane, we could saw that the type V is the smallest and the Type Flat is the largest. In clinical practice, when the internal fixation is implanted from the outside of the fibula, we observe the lateral MF before operation. If it is type V, the maximum depth of implantation at any angle outside the fibula can only be 8 mm. If it is the other two types, 9–10 mm can be selected, which is absolutely safe, but internal fixation instability may occur. After determining the type of the lateral MF, the most suitable depth can be selected when the lateral fibula is fixed, which can ensure the stability of the internal fixation and will not cause some unnecessary complications caused by the invasion of the lateral MF. In this study, such a length is absolutely safe. Another way to avoid damaging the lateral MF is to only go through the single cortex during implantation. Of course, selecting the most suitable implant is of great help to the healing of fractures.

This study has several limitations. Firstly, the sample size is small and it only has yellow people's information. Second, simple imaging data have certain errors, which may be more accurate in combination with anatomy. Future studies may be from anatomical or clinical research. This is a unique study in the medical literature—few studies on the classification of lateral MF. The clinical significance of the results requires further investigation. Analysis using imaging data alone needs to be more comprehensive.

Conclusion

According to the morphology of the CT cross section, the lateral MF was divided into three types: type C, type V and type Flat. Type V is most likely to be invaded when fixing the distal fibula. Screws less than 9 mm should be

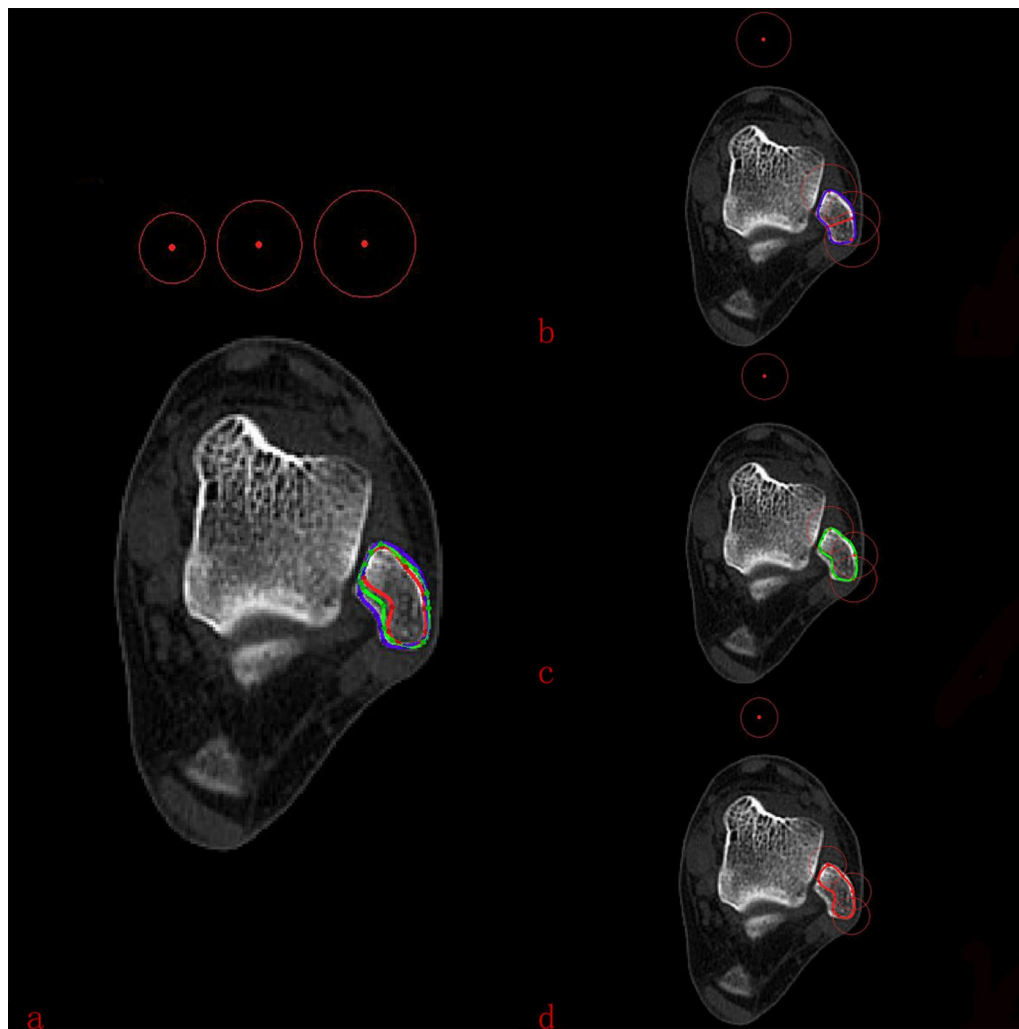


Fig. 5 Simulate the three types of different safety zones when the screw is placed from the outside to the inside. **a** Three types in a unified cross section on their safe area. **b** F type safety zone. **c** C safety zone. **d** V type safety zone

selected when fixing, and screws no more than 10 mm should be selected when there are other types of lateral MF.

Acknowledgements

Not applicable.

Author contributions

All authors contributed to the study conception and design. Material preparation, data collection and analysis were performed by LH and M-hL. The first draft of the manuscript was written by G-xY. BX, W-lP, H-yS prepared figures and tables. LZ made the critical revision of the manuscript. All authors read and approved the final manuscript.

Funding

This study was funded by National Natural Science Foundation of China (Youth Science Foundation Project), Project Number: 82004458. Scientific Research Cultivation Project of The Affiliated Traditional Chinese Medicine Hospital of Southwest Medical University, project number: 2022-CXTD-08. Supported by Sichuan Science and Technology Program, project number: 2022YFS0609. Hejiang People's Hospital—Southwest Medical University Science and Technology Strategic Cooperation Project (major project), Project Number: 2022HJXNYD04. General Project of Sichuan Traditional Chinese Medicine Administration Traditional Chinese Medicine Research Special Project (Fundamentals of Traditional Chinese Medicine), Project Number: 2023MS248.

Availability of data and materials

The datasets used and analyzed during the current study are available from the first author on a reasonable request and upon completing a data sharing agreement. The data are not publicly available due to inclusion of unique health information from participants in a specific and limited region that could compromise participant confidentiality.

Declarations

Ethics approval and consent to participate

This study was approved by the Affiliated Traditional Chinese Medicine Hospital of Southwest Medical University, Ethics Committee of our hospital (BY2022023), and written informed consent was obtained from all patients.

Consent for publication

Not applicable.

Competing interests

The authors declare they have no competing interests. No benefits in any form have been or will be received from a commercial party related directly or indirectly to the subject of this article.

Received: 7 August 2023 Accepted: 12 September 2023

Published online: 22 September 2023

References

- Gupton M, Munjal A, Kang M. Anatomy, bony pelvis and lower limb: fibula. In: StatPearls. Treasure Island: StatPearls Publishing; 2023.
- Matsui K, Oliva XM, Takao M, et al. Bony landmarks available for minimally invasive lateral ankle stabilization surgery: a cadaveric anatomical study. *Knee Surg Sports Traumatol Arthrosc.* 2017;25(6):1916–24. <https://doi.org/10.1007/s00167-016-4218-7>.
- Gandhi SD, Cross J, Siljander M, et al. Dimensions of the lateral malleolar fossa and its potential violation with lateral distal fibular plate fixation. *Orthopedics.* 2020;43(3):e141–6. <https://doi.org/10.3928/01477447-20200213-04>.
- Clelland SJ, Chauhan P, Mandari FN. The epidemiology and management of tibia and fibula fractures at Kilimanjaro Christian Medical Centre (KCMC) in Northern Tanzania. *Pan Afr Med J.* 2016;25:51. <https://doi.org/10.11604/pamj.2016.25.51.10612>.
- Elseo R, Ostgaard SE, Larsen P. Population-based epidemiology of 9767 ankle fractures. *Foot Ankle Surg.* 2018;24(1):34–9. <https://doi.org/10.1016/j.fas.2016.11.002>.
- King CM, Hamilton GA, Cobb M, Carpenter D, Ford LA. Association between ankle fractures and obesity. *J Foot Ankle Surg.* 2012;51(5):543–7. <https://doi.org/10.1053/j.fas.2012.05.016>.
- Sarpong NO, Levitsky M, Held M, Coury J, Greisberg J, Vosseller JT. Isolated fibular stress fractures: radiographic parameters. *Foot Ankle Surg.* 2020;26(8):935–8. <https://doi.org/10.1016/j.fas.2019.12.004>.
- Mitchell JJ, Bailey JR, Bozzio AE, Fader RR, Mauffrey C. Fixation of distal fibula fractures: an update. *Foot Ankle Int.* 2014;35(12):1367–75. <https://doi.org/10.1177/1071100714555712>.
- Marazzi C, Wittauer M, Hirschmann MT, Testa EA. Minimally invasive plate osteosynthesis (MIPO) versus open reduction and internal fixation (ORIF) in the treatment of distal fibula Danis-Weber types B and C fractures. *J Orthop Surg Res.* 2020;15(1):491. <https://doi.org/10.1186/s13018-020-02018-5>.
- Knutsen AR, Sangiorgio SN, Liu C, et al. Distal fibula fracture fixation: biomechanical evaluation of three different fixation implants. *Foot Ankle Surg.* 2016;22(4):278–85. <https://doi.org/10.1016/j.fas.2016.08.007>.
- Giordano V, Azevedo PH, Peres C, et al. Can CT-based assessment of lateral malleolus anatomy indicate when and how to perform an intramedullary fixation in distal fibula fractures? An analysis of 150 ankles. *Eur J Orthop Surg Traumatol.* 2023;33(3):601–9. <https://doi.org/10.1007/s00590-022-03360-6>.
- Bazin I, Armendariz M, Marcheix PS, et al. A computed tomography study of the fibula: morphology, morphometry, intramedullary anatomy, application prospects on intramedullary nailing. *Surg Radiol Anat.* 2019;41(6):681–7. <https://doi.org/10.1007/s00276-019-02213-y>.
- Fojtík P, Kostlivý K, Bartoníček J, Naňka O. The fibular notch: an anatomical study. *Surg Radiol Anat.* 2020;42(10):1161–6. <https://doi.org/10.1007/s00276-020-02476-w>.
- Fojtík P, Kašper Š, Bartoníček J, Tuček M, Naňka O. Lateral malleolar crest and its clinical importance. *Surg Radiol Anat.* 2023;45(3):255–62. <https://doi.org/10.1007/s00276-023-03080-4>.
- Hattori S, Onishi K, Yano Y, et al. Sonographically guided anchor placement in anterior talofibular ligament repair is anatomic and accurate. *Orthop J Sports Med.* 2020;8(12):2325967120967322. <https://doi.org/10.1177/2325967120967322>.
- Friesgaard KD, Gromov K, Knudsen LF, Brix M, Troelsen A, Nikolajsen L. Persistent pain is common 1 year after ankle and wrist fracture surgery: a register-based questionnaire study. *Br J Anaesth.* 2016;116(5):655–61. <https://doi.org/10.1093/bja/aew069>.
- Regan DK, Gould S, Manoli A 3rd, Egol KA. Outcomes over a decade after surgery for unstable ankle fracture: functional recovery seen 1 year post-operatively does not decay with time. *J Orthop Trauma.* 2016;30(7):e236–41. <https://doi.org/10.1097/BOT.0000000000000571>.

Publisher's Note

Springer Nature remains neutral with regard to jurisdictional claims in published maps and institutional affiliations.

Ready to submit your research? Choose BMC and benefit from:

- fast, convenient online submission
- thorough peer review by experienced researchers in your field
- rapid publication on acceptance
- support for research data, including large and complex data types
- gold Open Access which fosters wider collaboration and increased citations
- maximum visibility for your research: over 100M website views per year

At BMC, research is always in progress.

Learn more biomedcentral.com/submissions

